As noted above, $\alpha > 0.5$ is actually "anomalous" for any reaction having $\Delta G° < 0$ if one assumes a constant intrinsic barrier, but such reactions may be readily reconciled with a nonzero B parameter in the variable intrinsic barrier of eq 2. In this sense, Bordwell's conjecture[44] —that the deprotonation of ketones may resemble nitroalkane deprotonations in having unusual Brønsted α values—is fulfilled, since hydroxide ion catalyzed deprotonations of such ketones display B values in the range 0.18–0.32 (Table II) even though α is not greater than 1 as is found for phenylnitromethanes.

Acknowledgment. We thank Professor A. J. Kresge for discussions of this work and Professor M. M. Kreevoy for comments which encouraged us to present more than a strictly algebraic interpretation of eq 3 and its first derivatives. We appreciate the support of this work through an Operating Grant to J.W.B. from the Natural Sciences and Engineering Research Council of Canada and an Ontario Graduate Fellowship awarded to D.S.

(44) Bordwell, F. G.; Boyle, W. J., Jr.; Hautala, J. A.; Yee, K. C. *J. Am. Chem. Soc.* **1969**, *91*, 4002.

Thermal Decomposition of Allylbenzene Ozonide

James C. Ewing, Daniel F. Church, and William A. Pryor*

Contribution from the Biodynamics Institute and the Department of Chemistry, 711 Choppin Hall, Louisiana State University, Baton Rouge, Louisiana 70803. *Received August 22, 1988. Revised Manuscript Received March 18, 1989*

Abstract: Thermal decomposition of allylbenzene ozonide (ABO) at 98 °C in the liquid phase yields toluene, bibenzyl, phenylacetaldehyde, formic acid, and (benzyloxy)methyl formate as major products; benzyl chloride is formed when chlorinated solvents are employed. These products, as well as benzyl formate, are formed when ABO is decomposed at 37 °C. When the decomposition of ABO is carried out in the presence of 1-butanethiol, the product distribution changes: yields of toluene increase, no bibenzyl is formed, and decreases in yields of (benzyloxy)methyl formate, phenylacetaldehyde, and benzyl chloride are observed. The decomposition of 1-octene ozonide (OTO) also was studied for comparison. The activation parameters for both ABO and OTO are similar (28.2 kcal/mol, log A = 13.6 and 26.6 kcal/mol, log A = 12.5, respectively); these data suggest that ozonides decompose by homolysis of the O–O bond, rather than by an alternative synchronous two-bond scission process. When ABO is decomposed at 37 °C in the presence of the spin traps 5,5-dimethyl-1-pyrroline N-oxide (DMPO) or 3,3,5,5-tetramethyl-1-pyrroline N-oxide (M_4PO), ESR signals are observed that are consistent with the trapping of benzyl and other carbon- and oxygen-centered radicals. A mechanism for the thermal decomposition of ABO that involves peroxide bond homolysis and subsequent β-scission is proposed. Thus, Criegee ozonides decompose to give free radicals at quite modest temperatures.

The reaction of ozone with olefins has been the subject of intense study.[1] The generally accepted mechanism for the ozonation of simple olefins in the liquid phase is that proposed by Criegee[2] and modified by others.[3] It involves the formation of a 1,2,3-trioxolane, **1**, which undergoes rapid scission to give a carbonyl oxide,

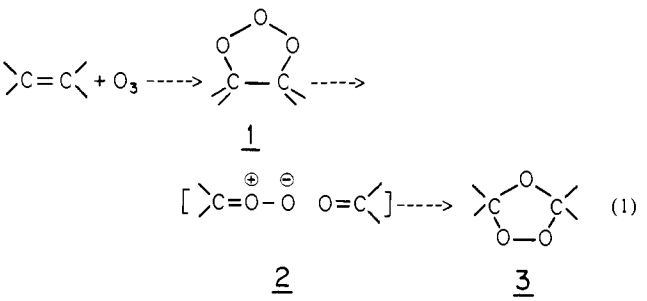

2, and a carbonyl compound. In the absence of a protic solvent, **2** reacts rapidly with a carbonyl compound to yield a 1,2,4-trioxolane, **3**; **3** is commonly called the Criegee ozonide.[1] Even though this mechanism does not involve free radicals, evidence collected over recent years implicates radicals as reactive intermediates in the ozonation of some olefins.[1,4]

Our efforts have been aimed at elucidating the mechanism(s) by which ozone, a nonradical, reacts with olefins to produce radicals.[4d-h] As part of this study we have examined the reaction of ozone with polyunsaturated fatty acids (PUFA) and model PUFA compounds.[4d-h] We recently utilized allylbenzene, **4** as

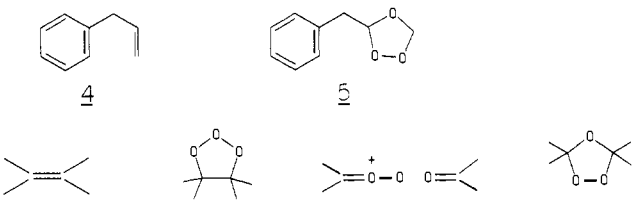

a PUFA model and showed that allylbenzene ozonide (ABO), **5**, initiates the autoxidation of methyl linoleate (18:2ME) at 37 °C.[5]

(1) Bailey, P. S. *Ozonation in Organic Chemistry*; Academic Press: New York, 1978; Vol I.

(2) (a) Criegee, R. *Liebigs Ann. Chem.* **1953**, *583*, 1–36. (b) Criegee, R. In *Peroxide Reaction Mechanisms*; Edwards, J. D., Ed.; Wiley-Interscience: New York, 1962.

(3) (a) Huisgen, R. *Angew. Chem., Int. Ed. Engl.* **1963**, *2*, 565–598. (b) Greenwood, F. L.; Rubenstein, H. *J. Org. Chem.* **1969**, *32*, 3369–3374.

(4) (a) Pryor, W. A.; Dooley, M. M.; Church, D. F. In *The Biomedical Effects of Ozone and Related Photochemical Oxidants*; Lee, S. D., Mustafa, M. G., Mehlman, M. A., Eds.; Princeton Scientific Publishers: Princeton, NJ, 1982; pp 7–19. (b) Menzel, D. B. In *Free Radicals in Biology*; Pryor, W. A., Ed.; Academic Press: New York, 1976; Vol. II, pp 181–202. (c) Pryor W. A. In *Free Radicals in Biology*; Pryor, W. A., Ed.; Academic Press: New York, 1982; Vol. I, pp 1–49. (d) Pryor, W. A.; Stanley, J. P.; Blair, E.; Cullen, G. B. *Arch. Environ. Health* **1976**, *31*, 201–210. (e) Pryor, W. A.; Prier, D. G.; Church, D. F. *Environ. Res.* **1981**, *24*, 42–52. (f) Pryor, W. A.; Prier, D. G.; Church, D. F. *J. Am. Chem. Soc.* **1983**, *105*, 2883–2888. (g) Pryor, W. A.; Gu, J.; Church, D. F. *J. Org. Chem.* **1985**, *50*, 185–189. (h) Pryor, W. A.; Ohto, N.; Church, D. F. *J. Am. Chem. Soc.* **1983**, *105*, 3614–3622.

(5) (a) Ewing, J. C.; Cosgrove, J. P.; Giamalva, D. G.; Church, D. F.; Pryor, W. A. *Lipids*, in press. (b) Ewing, J. C. Ph.D. Dissertation, Louisiana State University, 1988; pp 1–78.

0002-7863/89/1511-5839$01.50/0

In this paper we report an extension of that work and present data on the thermal decomposition of ABO and 1-octene ozonide (OTO) in the liquid phase.[6]

Experimental Section

Instrumentation. Gas chromatography (GC) analyses were performed on a Varian 3700 gas chromatograph equipped with a 0.25 mm × 30 m DB-5 capillary column (J&W Scientific, fused silica) and a flame ionization detector. Peak areas were converted to molar units by using response factors relative to an internal standard (chlorobenzene). Mass spectra (electron impact (EI) at 70 eV) were obtained with a Hewlett-Packard 5970 gas chromatograph–mass spectrometer (GC-MS) equipped with a 0.20 mm × 30 m dimethylsilicone cross-linked capillary column (Hewlett-Packard). Proton and carbon nuclear magnetic resonance (^{1}H and ^{13}C NMR) spectra were obtained at 400, 200, and 100 MHz with Bruker 400-AM, Bruker WP-200, and IBM NR/100 model spectrometers, respectively; all chemical shifts are expressed relative to $(CH_3)_4Si$. Infrared (IR) spectra were recorded with an IBM IR/32 FT-IR spectrometer. UV–vis analyses were carried out using a Hewlett-Packard 8451A diode array spectrophotometer. Quantitative high-pressure liquid chromatography (HPLC) analyses were performed with a Hewlett-Packard 1090 liquid chromatograph equipped with a diode array UV–vis detector; all analyses utilized a Du Pont cyanopropyl column (4.9 mm × 25 cm) using hexane/diethyl ether (99:1) at 1 mL min^{-1}. Semipreparative HPLC was carried out on a Varian 5000 liquid chromatograph equipped with a Varian UV50 variable-wavelength detector and a Whatman silica column (9.4 mm × 50 cm) using isocratic combinations of hexane/diethyl ether at 3.5 mL min^{-1}. Electron spin resonance (ESR) spectra were recorded with either a Bruker ER-200 or a Varian E-109 ESR spectrometer.

General Ozonolysis Procedure. Ozone was delivered as an ozone/oxygen stream at a rate of 0.1–0.2 mmol of ozone min^{-1}; the ozone in the gas stream was measured by the method of Birdsall and co-workers.[7] Ozonolysis was typically carried out at −78 °C to about 90% of the theoretical requirement of olefin. **CAUTION**: Due to the possibility of detonation, all ozonation mixtures, as well as purified ozonides, should be handled behind a safety shield and with thick gloves.

Materials. Allylbenzene (Aldrich, 98%) and 1-octene (Aldrich, 99%) were distilled under reduced pressure and passed through neutral alumina immediately before ozonation. Toluene (99%), bibenzyl (99%), benzyl chloride (97%), benzyl chloromethyl ether, 1-butanethiol (99%), chlorobenzene (99.9%), 5,5-dimethyl-1-pyrroline *N*-oxide (DMPO, 97%), 3,3,5,5-tetramethyl-1-pyrroline *N*-oxide (M_4PO, 97%), and sodium formate (99%) were purchased from Aldrich and used without further purification. Phenylacetaldehyde (Lancaster Synthesis, 98%) was purified by semipreparative HPLC. Formic acid was obtained by azeotropic distillation of an 88% solution obtained commercially (Fisher). Formaldehyde was generated by heating paraformaldehyde (Mallinckrodt) in a stream of N_2. Dibenzylmercury (95%, Pfaltz and Bauer) and benzyl formate (98%, Alfa), were used as obtained.

Preparation of Allylbenzene Ozonide (ABO), 5, and 1-Octene Ozonide (OTO), 9. The preparation of **5** was carried out as described elsewhere.[5] The synthesis of OTO was carried out as follows.[6] A solution of 1-octene (1 mL, 6 mmol) in 4 mL of hexane was ozonized by the general procedure, flushed with N_2 at −78 °C, and warmed to room temperature. Excess hexane was removed in vacuo; 0.2 g of the resulting crude residue was eluted on silica (30 × 1.5 cm) with hexane, and the fraction corresponding to the ozonide was collected. Pure OTO was obtained as a colorless and transparent liquid. ^{1}H NMR ($CDCl_3$) δ 0.89 (t, 3 H), 1.50 (m, 10 H), 5.03 (s, 1 H), 5.13 (t, 1 H), 5.20 (s, 1 H); ^{13}C NMR ($CDCl_3$) δ 14.00, 22.47, 23.79, 29.03, 31.09, 31.59, 93.98, 103.86 ppm; IR (thin film) 2930, 1105, 1059 cm^{-1}. Anal. Calcd for $C_8H_{16}O_3$: C, 59.98; H, 10.07. Found: C, 60.00; H, 10.10.

The ^{1}H NMR chemical shifts of the ozonide ring protons of OTO (5.03, 5.13, 5.20 ppm, respectively) are in good agreement with ^{1}H NMR chemical shifts reported by Diaper[8] for 1-decene ozonide (5.01, 5.13, and 5.15 ppm).

Preparation of (Benzyloxy)methyl formate. This procedure is similar to a procedure reported by Clark and co-workers.[9] A solution of benzyl chloromethyl ether (1.7 mL, 12 mmol) in 10 mL of THF was added dropwise under N_2 to a stirred suspension of sodium formate (1 g, 15 mmol) in 20 mL of THF at 0 °C. Excess THF was removed under a stream of N_2, and the reaction mixture was refluxed for 6 h. Isolation of the pure compound was accomplished by semipreparative HPLC. Purified (benzyloxy)methyl formate (0.3 g, 15% yield) was obtained as a colorless and transparent liquid: ^{1}H NMR ($CDCl_3$) δ 4.72 (s, 2 H), 5.43 (s, 2 H), 7.34 (m, 5 H), 8.15 ppm (s, 1 H); ^{13}C NMR ($CDCl_3$) δ 71.93, 88.04, 127.9, 128.2, 128.5, 136.5, 160.5 ppm; IR (thin film) 1732, 1262, 1167, 1192, 741, 698 cm^{-1}; UV (hexane) 258 nm. Anal. Calcd for $C_9H_{10}O_3$: C, 65.05; H, 6.07. Found: C, 64.69; H, 6.13.

Product Studies. Quantitative analyses of products obtained from the thermal decomposition of ABO were typically carried out as follows. Into a 2-mL ampule were weighed 0.0113 g (68 μmol) of ABO; 1.00 mL of solvent was then added, and this solution was sealed at −78 °C under N_2 purge. After being heated at 98 ± 1 °C for 1.5 h, the contents of the ampule were quantitatively transferred to a 10.00-mL volumetric flask containing a known amount of chlorobenzene (usually 13 μmol) and diluted to 10.00 mL with hexane/diethyl ether (10:1). Triplicate analyses by capillary GC were then performed. A typical temperature program consisted of a 4-min hold at 40 °C followed by a 12 °C min^{-1} ramp to 280 °C. Formic acid was quantitated by titration with standard NaOH by using phenolphthalein as an indicator.

A separate set of experiments was conducted in a manner identical with that above with the following exception: to each of three ampules containing 0.0113 g (68.1 μmol) of ABO in 1.00 mL of $CDCl_3$ were added 7.0 μL (65 μmol), 11 μL (100 μmol), or 23 μL (220 μmol) of 1-butanethiol.

Decomposition runs were also performed at 37 °C by using 0.0057 g (34 μmol) of ABO in 0.5 mL of $CDCl_3$ or CCl_4. These samples were heated at 37 °C for 86 days and then analyzed as described above.

All products except formic acid and formaldehyde were isolated from fully decomposed ABO/$CDCl_3$ reaction mixtures by semipreparative HPLC and characterized by UV–vis, IR, ^{1}H and ^{13}C NMR, and GC–MS. These analytical data were compared to analytical data obtained for authentic samples; formic acid and formaldehyde were assigned on the basis of ^{1}H NMR alone. CO was assigned by comparing GC retention times of peaks obtained from head-space analysis with retention times of an authentic sample of CO under identical GC conditions.

ESR Studies. DMPO. To a 1-mL solution of DMPO in benzene-d_6 (0.1 M) was added 15 μL (100 μmol) of ABO to give a final ABO concentration of 0.1 M. A portion of this sample was then transferred to a quartz ESR tube, purged with Ar for 6 min, and tightly capped. After incubation at 37 °C for 15 min, the sample was analyzed at room temperature by ESR.

M_4PO. To a 0.5-mL solution of M_4PO in benzene-d_6 (0.1 M) was added 5.0 μL (34 μmol) of ABO to give a final ABO concentration of 7×10^{-2} M. This sample was transferred to a quartz ESR tube, purged with N_2, and tightly capped. After incubation at 37 °C for 30 min, the sample was analyzed at room temperature by ESR.

Benzyl radicals were produced and trapped in benzene-d_6 by using a modification of a method reported by Janzen and Blackburn.[10] Thus, a saturated solution of dibenzyl mercury in benzene-d_6 (about 0.02 M) was prepared by adding about 80 mg (20 μmol) of dibenzylmercury to 1 mL of benzene-d_6; the small amount of undissolved solid was separated by decantation. This alkylmercury solution was then mixed with a 1-mL benzene-d_6 solution of the appropriate spin trap (0.2 M), and an aliquot of this mixture was transferred to a quartz ESR tube, purged with Ar for 6 min, and tightly capped. These samples were then photolyzed in the cavity of the ESR spectrometer by using a 200-W Hg lamp equipped with a Corning 300-nm cutoff filter for about 5 min, and the ESR spectra were recorded.

Kinetics of OTO Decomposition. In a typical experiment 1.00-mL aliquots of stock solutions of OTO in CCl_4 were transferred to a series of 2-mL ampules that were then sealed under N_2 purge at −78 °C. Twenty-five ampules were thermostated at 50 °C; individual ampules were periodically withdrawn, and the disappearance of ozonide was measured over 3 half-lives by HPLC.

Results

Product Study. Table I lists the products identified from the thermal decomposition of ABO in various solvents at 98 or 37 °C under N_2. In general, the major products are toluene, bibenzyl, (benzyloxy)methyl formate, phenylacetaldehyde, benzyl chloride (when CCl_4 or $CDCl_3$ are used as solvents), and formic acid. Benzyl formate is observed when the decomposition is carried out at 37 °C. Formaldehyde is detected by ^{1}H NMR but has not been quantitated. Analysis of the head space above the decomposed mixture showed a 9% yield of CO; no CO_2 was detected. When

(6) See ref 5b, pp 79–165.
(7) Birdsall, C. M.; Jenkins, A. C.; Spandinger, E. *Anal. Chem.* **1952**, *24*, 662–664.
(8) Diaper, D. G. *Can. J. Chem.* **1968**, *46*, 3095–3098.
(9) Clark, F. E.; Cox, S. F.; Mack, E. *J. Am. Chem. Soc.* **1917**, *39*, 712–716.
(10) Janzen, E. G.; Blackburn, B. J. *J. Am. Chem. Soc.* **1969**, *91*, 4481–4490.

Table I. Mole Percentage[a] of Products from the Thermal Decomposition of Allylbenzene Ozonide (ABO) in the Absence of Oxygen

	yield, %						
	98 °C					37 °C	
products	$CDCl_3$[b]	CCl_4	CH_3CN	$(CH_3)_2CO$	hexane	$CDCl_3$	CCl_4
toluene	25 ± 2	16 ± 2	21 ± 2	16 ± 2	13 ± 1[c,d]	29 ± 1	18 ± 1
bibenzyl	5.6 ± 0.4	1.0 ± 0.3	7 ± 1	8.6 ± 0.4	4.5 ± 0.2[c,d]	3.0 ± 0.1	0.17 ± 0.05
(benzyloxy)methyl formate	16 ± 2	14 ± 1	12 ± 1	12 ± 1	12 ± 1[c,d]	4.9 ± 0.3	13 ± 1
phenylacetaldehyde	21 ± 2	29 ± 1	28 ± 2	33 ± 3	43 ± 2[d]	6.0 ± 0.2	19 ± 1
benzyl chloride	3.6 ± 0.4	11 ± 1	NO[e]	NO	NO	10 ± 1	11 ± 1
benzyl formate	NO	NO	NO	NO	NO	9.1 ± 0.5	5.8 ± 0.5
formic acid	84 ± 7	ND[f]	79 ± 5	ND	83 ± 4	ND	ND
total % benzyl mass[g]	77 ± 7	72 ± 6	75 ± 6	78 ± 6	77 ± 5	65 ± 3	67 ± 4

[a] Based on initial ABO ((6.8 ± 0.2) × 10^{-5} mol) except for the 37 °C runs; these percent yields are based on (3.4 ± 1) × 10^{-5} mol of ABO. The error associated with each entry are average deviations. [b] In addition to the listed products, CO was formed in 9 ± 3 % yield. [c] Verified by HPLC. [d] These yields are independent of ABO concentration over the range 3.6–14 mM. [e] Not observed. [f] Not determined. [g] Only products containing a benzyl group and assuming 1 mol of bibenzyl per 2 mol of ABO.

Table II. Mole Percentage[a] of Products from the Thermal Decomposition of ABO in the Absence and Presence of 1-Butanethiol at 98 °C

	solvent	
product	$CDCl_3$	$CDCl_3$ + 1-butanethiol[b]
toluene	25 ± 2	44 ± 1
bibenzyl	5.6 ± 0.4	NO[c]
(benzyloxy)methyl formate	16 ± 2	10 ± 1
phenylacetaldehyde	21 ± 2	11.0 ± 0.3
benzyl chloride	3.6 ± 0.4	2.8 ± 0.3
benzyl formate	NO	NO
formic acid	84 ± 7	ND[d]
total % "benzyl mass"[e]	77 ± 7	68 ± 3

[a] Based on initial ABO ((6.8 ± 0.2) × 10^{-5} mol). [b] Product yields independent of 1-butanethiol concentration between 65 and 215 mM; Δ[1-butanethiol] = (5.2 ± 0.2) × 10^{-5} M. [c] Not observed. [d] Not determined. [e] Only products containing a benzyl group and assuming 1 mol of bibenzyl per 2 mol of ABO.

Table III. Rate Constants for the Thermal Decomposition of 1-Octene Ozonide (OTO) in CCl_4 under N_2 in the Presence of 1-Butanethiol

OTO, mM	1-Butanethiol, mM	temp, °C	$10^6 k_d$[a]
61.9	80.5	50	3.8 ± 0.1
61.9	80.5	70	36.7 ± 0.9
65.6	86.1	70	36.1 ± 0.9
61.9	80.5	98	790 ± 30
65.6	86.1	98	750 ± 15

[a] Obtained by least-squares analysis of data fit to the equation log (OTO) = $-k_d t/2.303$, where (OTO) is the raw peak area from HPLC analysis, t is time, and the slope of the line is equal to $-k_d/2.303$. Units are s^{-1} (±standard deviation).

the decomposition of ABO is carried out in the presence of 1-butanethiol, the product distribution changes (Table II): yields of toluene increase, no bibenzyl is formed, and decreases in yield of (benzyloxy)methyl formate, phenylacetaldehyde, and benzyl chloride are observed.

Kinetics of the Thermal Decomposition of ABO and OTO. We have reported rate constants for the thermal decomposition of ABO elsewhere.[5] For purposes of comparison, rate constants for the thermal decomposition of OTO were obtained in an identical fashion. In the presence of the radical scavenger 1-butanethiol, decomposition is first order in OTO over at least 3 half-lives; rate constants obtained at 50, 70, and 98 °C are listed in Table III. From these rate data, an Arrhenius plot can be constructed (Figure 1) from which activation parameters E_a = 26.6 ± 0.5 kcal mol^{-1} and log A = 12.5 ± 0.3 are obtained. These parameters are compared to E_a = 28.2 ± 0.3 kcal mol^{-1} and log A = 13.6 ± 0.2 for ABO.[5]

Spin Trapping Authentic Benzyl Radicals with DMPO or M_4PO. The photolysis of dibenzylmercury in benzene-d_6 containing DMPO produced a doublet of triplets with hyperfine splitting

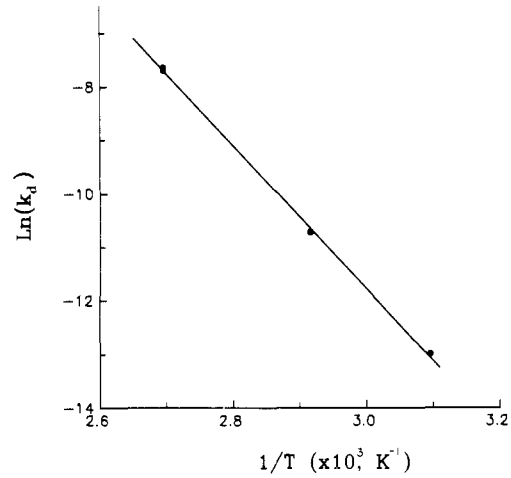

Figure 1. Arrhenius plot for the thermal decomposition of 64 ± 2 mM 1-octene ozonide (OTO) in the presence of 83 ± 3 mM 1-butanethiol. The slope of the line equals $-E_a/R$, where R = 1.987 cal mol^{-1} K^{-1} and the intercept is ln A. Data are from Table III.

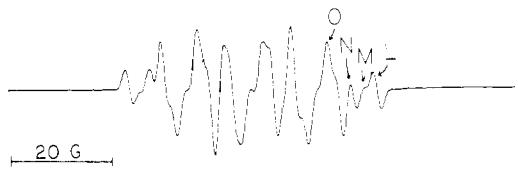

Figure 2. ESR spectrum obtained by heating a benzene-d_6 solution of 0.1 M ABO and 0.1 M DMPO at 37 °C for 15 min in the absence of oxygen. The ESR conditions are microwave power, 15 mW; modulation amplitude, 1 G; gain, 8 × 10^4; center field, 3478 G; sweep width, 100 G; sweep time, 0.8 min, number of scans, 10. Signals L–O are discussed in Table IV.

constants (hfsc) of a_N = 14.15 ± 0.06 G and $a_{H(1)}$ = 20.65 ± 0.02 G. These hfsc are in good agreement with hfsc reported by Janzen and Liu for a benzyl radical–DMPO spin adduct (a_N = 14.16 G and $a_{H(1)}$ = 20.66 G).[11] Similarly the photolysis of dibenzylmercury in benzene containing M_4PO produced a doublet of triplets with hfsc of a_N = 14.6 ± 0.1 G and $a_{H(1)}$ = 24.2 ± 0.1 G; the ESR spectrum of a benzyl radical–M_4PO spin adduct had not been previously reported.

Thermal Decomposition of ABO in the Presence of DMPO or M_4PO.[12] When 0.1 M ABO in benzene-d_6 is warmed to 37 °C

(11) (a) Janzen, E. G.; Liu, J. I. *J. Magn. Reson.* **1973**, 9, 510–512.

(12) We have performed some experiments in which sealed samples of ABO in $CDCl_3$ were heated to 100 °C in the probe of a 200-MHz NMR spectrometer;[6] we did not observe chemically induced dynamic nuclear polarization (CIDNP) effects[13] at any of the ^1H NMR signals corresponding to the products listed in Table I. The reasons for this may be due to (1) an insufficient rate of formation of radicals and/or (2) lack of sufficient singlet–triplet mixing between radical pairs.[13c] The CIDNP method was thus abandoned in favor of the ESR spin-trapping method.

Table IV. ESR Hfsc[a] for DMPO Spin Adducts L, M, N, and O (Figure 2) Obtained from Warming Benzene-d_6 Solutions of ABO (0.1 M) to 37 °C in the Presence of 0.1 M DMPO

adduct	a_N	$a_{H(1)}$	$a_{H(2)}$	spectral width[b]	assignt
L	14.1 ± 0.1	20.7 ± 0.1			benzyl
M[c]	14.0	16.7			acyl
N	unresolved[d]			39.9 ± 0.1[e]	NA[f]
O[c]	13.0	7.1	1.7		oxygen centered

[a] Values are expressed in gauss ± average deviations and are measured from the second derivative ESR spectra except where noted. [b] Spectral width = $2a_N + a_{H(1)} + a_{H(2)}$. [c] Hyperfine splitting constants were determined by computer stick simulation. [d] Not resolved due to an insufficient number of lines. [e] The spectral width was measured directly from Figure 2. [f] Not assigned.

Table V. ESR Hyperfine Parameters[a] for M_4PO Spin Adducts P, Q, and R (Figure 3) Obtained from Warming 7×10^{-2} M ABO to 37 °C in the Presence of 0.1 M M_4PO in Benzene[b]

adduct	a_N	$a_{H(1)}$	assignt
P	14.8 ± 0.3	24.4 ± 0.5	benzyl
Q	14.0 ± 0.3	11.9 ± 0.3	oxygen centered
R	13.6 ± 0.3	6.0 ± 0.3	alkoxyl

[a] These hfsc were determined by peak-to-peak measurements from Figure 3; all values are expressed in gauss ± average deviations.

under Ar in the presence of 0.1 M DMPO, ESR signals are observed; these are shown in Figure 2. Table IV lists the hfsc for spin adducts L, M, N, and O. Spin adduct L is assigned as a benzyl radical adduct of DMPO on the basis of the following observations: (1) the hfsc (a_N = 14.1 ± 0.1 G and $a_{H(1)}$ = 20.7 ± 0.1 G) are in good agreement with both our experimentally determined hfsc for a benzyl radical–DMPO spin adduct (a_N = 14.15 ± 0.06 G and $a_{H(1)}$ = 20.65 ± 0.02 G) and Janzen and Liu's hfsc (a_N = 14.16 G and $a_{H(1)}$ = 20.66 G)[11] and (2) ABO decomposes at 37 °C to yield products that are consistent with intermediate benzyl radicals (see the Discussion). The hfsc for spin adduct M (a_N = 14.0 G and $a_{H(1)}$ = 16.7 G) are consistent with an acyl radical spin adduct;[11,14] however, the exact structure of this radical is unknown. Hyperfine splitting constants for DMPO spin adduct O (a_N = 13.0 G, $a_{H(1)}$ = 7.1 G, and $a_{H(2)}$ = 1.7 G) are consistent with an oxygen-centered radical.[11,14] The ESR spectrum of spin adduct N is unresolved; the spectral width (39.9 ± 0.1 G) is intermediate between spectral widths for oxygen- and carbon-centered adducts,[11,14] and therefore the structure of spin adduct N is not assigned.

Spin trapping was also performed using 3,3,5,5-tetramethyl-1-pyrroline *N*-oxide (M_4PO) as the spin trap. When 7×10^{-2} M ABO in benzene is warmed to 37 °C under N_2 in the presence of 0.1 M M_4PO, the ESR signals shown in Figure 3 are observed. The ESR spectrum consists of three overlapping doublets of triplets, P, Q, and R; hfsc for each of these spin adducts are listed in Table V. We assign spin adduct P to a benzyl radical adduct of M_4PO based on a favorable comparison of the hfsc (a_N = 14.8 ± 0.3 G and $a_{H(1)}$ = 24.4 ± 0.5 G) to our experimentally determined hfsc for a benzyl radical–M_4PO spin adduct (a_N = 14.6 ± 0.1 G and $a_{H(1)}$ = 24.2 ± 0.1 G). Spin adduct R has hfsc (a_N = 13.6 ± 0.3 G and $a_{H(1)}$ = 6.0 ± 0.3 G) that are consistent with an alkoxyl spin adduct.[14a,d,15,16] Hyperfine splitting constants for spin adduct Q (a_N = 14.0 ± 0.3 G and $a_{H(1)}$ = 11.9 ± 0.3 G) are intermediate between those reported for oxygen- and carbon-centered M_4PO spin adducts.[14a,d,15,16] Although a definite assignment cannot be made with the available data, we tentatively assign Q as an oxygen-centered spin adduct since the β-hyperfine of Q is more consistent with the β-hyperfine reported for oxygen-centered M_4PO spin adducts.[14a,d,15,16]

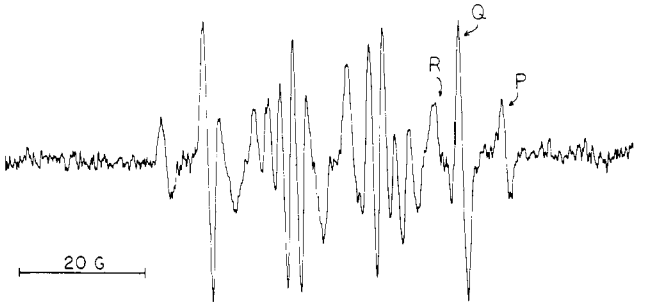

Figure 3. ESR spectrum obtained by heating a benzene-d_6 solution of 0.07 M ABO and 0.1 M M_4PO at 37 °C for 30 min in the absence of oxygen. ESR conditions are microwave power, 10 mW; modulation amplitude, 1 G; gain, 2.5×10^4; center field, 3350 G; sweep width, 100 G; sweep time, 4 min; number of scans, 1. Signals P, Q, and R are discussed in Table V.

Discussion

Table I lists the products obtained when ABO is thermally decomposed at 98 or 37 °C in the absence of oxygen. A mechanism that accounts for these products is presented in Scheme I. Previous workers have suggested that the thermal decomposition of Criegee ozonides proceed via initial ozonide peroxide bond homolysis.[17] The first step of our mechanism (path a) involves the unimolecular homolysis of the ABO peroxide bond to yield the oxy diradical **6**. Our experimentally determined activation energy of 28.2 ± 0.3 kcal mol^{-1} is in reasonable agreement with Benson's estimate of 30 kcal mol^{-1} for ozonide homolysis.[18] The log preexponential factor of 13.6 ± 0.2, however, is less than the expected value of 15–16 for a unimolecular decomposition.[19] This low preexponential factor could be rationalized if the ozonide peroxide bond homolysis proceeded with some degree of concertedness with β-scission of the adjacent benzyl group, as shown in eq 2. Transition state **8** shows spin delocalization onto the

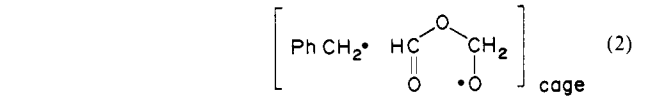

(2)

adjacent benzyl substituent; this stabilization would require some restrictions of motion to ensure favorable orbital overlap. The consequence of this more "ordered" transition state would be a smaller Arrhenius preexponential factor.[20a] To test this expla-

(13) (a) Kaptein, R.; Oosterhoff, L. J. *Chem. Phys. Lett.* **1969**, *4*, 214–216. (b) Closs, G. L. *J. Am. Chem. Soc.* **1969**, *91*, 4552–4554. (c) Kaptein, R. In *Advances in Free Radical Chemistry*; Elek Science: London, 1975; Vol. V, pp 319–380.

(14) (a) Haire, D. L.; Janzen, E. G. *Can. J. Chem.* **1982**, *60*, 1514–1522. (b) Davies, M. J.; Slater, T. F. *Biochem. J.* **1986**, *240*, 789–795. (c) Augusto, O.; Kunze, K. L.; de Montellano, P. R. *J. Biol. Chem.* **1982**, *257*, 6231–6241. (d) Huie, R. Ph.D. Dissertation, Louisiana State University, 1987. (e) Hill, H. A. O.; Thonalley, P. J. *FEBS Lett.* **1981**, *125*, 235–238.

(15) Janzen, E. G.; Shetty, R. V.; Kunanec, S. M. *Can. J. Chem.* **1981**, *59*, 756–758.

(16) Alberti, A.; Leardini, R.; Pedulli, G. F.; Tundo, A.; Zanardi, G. *Gazz. Chim. Ital.* **1983**, *113*, 869–871.

(17) (a) Hull, L. A.; Hisatsune, I. C.; Heicklen, J. *J. Phys. Chem.* **1972**, *76*, 2659–2665. (b) Bernatek, E.; Hvatum, M. *Acta Chem. Scand.* **1960**, *14*, 836–840. (c) Privett, O. S.; Nickell, E. C. *J. Am. Oil Chem. Soc.* **1966**, *43*, 393–400. (d) Nickell, E. C.; Privett, O. S. *Lipids* **1965**, *1*, 166–170. (e) Story, P. R.; Hall, T. K.; Morrison, W. H.; Farine, J. C. *Tetrahedron Lett.* **1968**, *52*, 5397–5400. (f) Story, P. R.; Morrison, M. H.; Hall, T. K., Farine, J. C.; Bishop, C. E. *Tetrahedron Lett.* **1968**, 3291–3294.

(18) Benson, S. W. In *Thermochemical Kinetics*, 2nd ed.; Wiley: New York, 1976; p 268.

(19) See ref 18, p 97.

(20) (a) Bartlett, P. D.; Hiatt, R. R. *J. Am. Chem. Soc.* **1958**, *80*, 1398–1405. (b) In their study on the rates of decomposition of substituted peresters ($RC(O)OOC(CH_3)_3$), Bartlett and Hiatt[20a] report a 250-fold decrease in rate of decomposition by changing R from a benzyl to a methyl group.

Scheme I

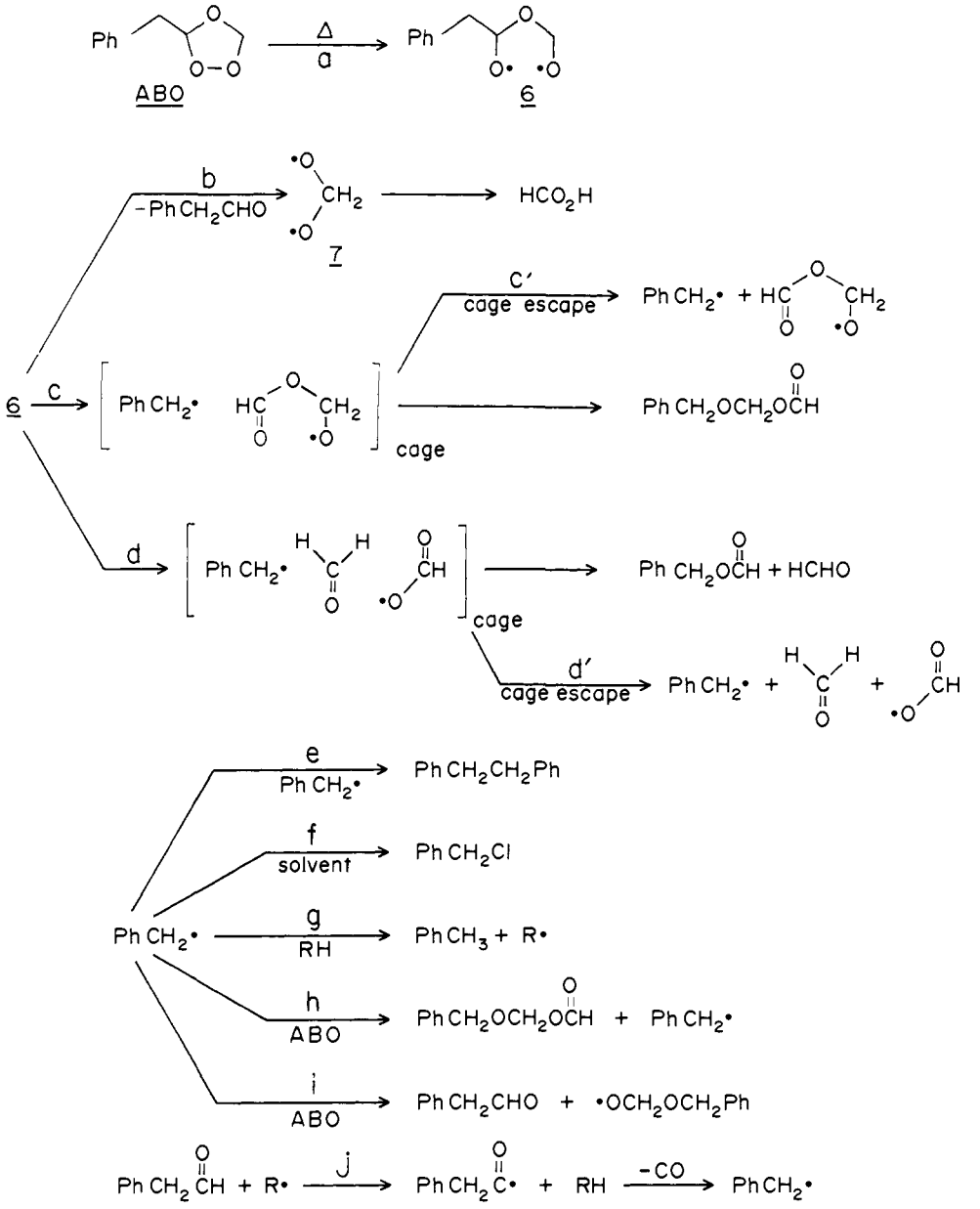

nation, the activation parameters for the thermal decomposition of OTO, **9**, were determined. If transition state **8** is important

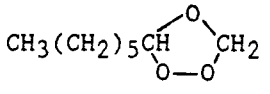

9

in the cleavage of the ozonide bond, then changing the adjacent alkyl group from a benzyl group to a primary *n*-alkyl group should slow the rate of thermal decomposition.[20b] Arrhenius activation parameters for OTO (E_a = 26.6 ± 0,5 kcal mol^{-1} and log A = 12.5 ± 0.3) are similar to those obtained for ABO; this finding appears to rule against a concerted process.

It must be remembered that a log preexponential factor of 15–16 is predicted for unimolecular reactions in the gas phase.[21] Since our reactions were performed in the liquid phase, our log A value of 13.6 ± 0.2 may reflect the effect of solvent reorganization in the transition state, leading to a "tighter" transition-state structure.[22] It is also possible that some induced decomposition occurs under the reaction conditions, and this would also lead to lower activation parameters.

The mechanism presented in Scheme I is different from the mechanism proposed by Story and co-workers[17e] and modified by Hull and co-workers[17a] for the thermal decomposition of diisopropyl ozonide **10**. Story and co-workers proposed an intramolecular hydrogen atom abstraction step after ozonide peroxide bond homolysis as shown in eq 3 and 4. Hull and co-workers modified

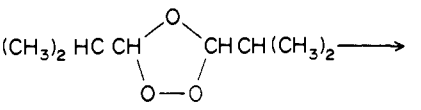

10

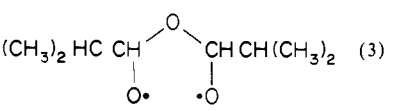

(3)

11

(21) See Ref 18, pp 78–140.

(22) Pryor, W. A.; Smith, K. *Int. J. Chem. Kinet.* **1971**, *3*, 387–394.

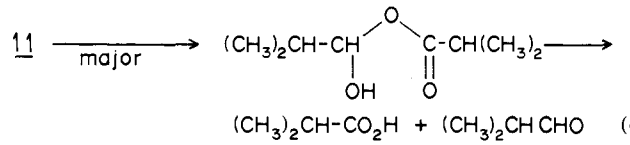

(4)

this mechanism to include concerted homolysis and intramolecular hydrogen atom abstraction as shown in eq 5.[17a] The toluene,

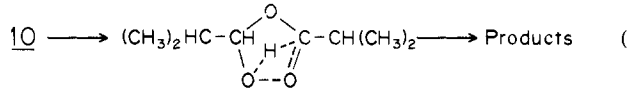

(5)

bibenzyl, (benzyloxy)methyl formate, benzyl chloride, and benzyl formate that we observe from the thermal decomposition of ABO cannot be rationalized in terms of the Story/Hull mechanism. To explain these products, we propose that the thermal decomposition of ABO involves initial ABO peroxide bond homolysis (Scheme I, path a) to yield the oxy diradical **6** followed by β-scission (Scheme I, paths b–d).

CO is formed in 9 ± 3% yield (Table I); a reasonable mechanism for its formation is shown as path j in Scheme I. This is similar to the mechanism proposed by Greiner and Muller[23] to explain the evolution of CO during the thermal decomposition of 1-octene ozonide.

With one exception, the products obtained from the thermal decomposition of ABO at 37 and 98 °C are the same; this suggests that the mechanism of decomposition changes little over this temperature range. Benzyl formate is formed when the decomposition is carried out at 37 °C, but it is not formed at 98 °C. Path d (Scheme I) shows a reasonable mechanism for the formation of benzyl formate that involves double β-scission of the oxy diradical **6** followed by cage recombination.[24]

Following a suggestion by Nangia and Benson,[25] formic acid is proposed to arise, in part, by pathway b (Scheme I) via the methylenebis(oxy) radical **7**; Nangia and Benson predict the isomerization of **7** to formic acid. Yields of formic acid are significantly greater than yields of phenylacetaldehyde (Table I); this implies that formic acid is formed by other, as yet unknown, pathway(s) and/or that formic acid is more stable toward further radical attack than is phenylacetaldehyde.[26]

Decomposition of ABO in the Presence of 1-Butanethiol. Thiols are very effective hydrogen atom donors and have been employed to investigate cage and/or chain processes in radical reactions.[24b] Table II shows the effect of 1-butanethiol on the product distribution obtained from the decomposition of ABO at 98 °C. Yields of toluene increase from 25 ± 2 to 44 ± 1% and bibenzyl is not observed when the decomposition is carried out in the presence of 1-butanethiol. In addition, yields of benzyl chloride decrease (Table II). These results are consistent with the scavenging of benzyl radicals by 1-butanethiol (eq 6). Yields of

$$PhCH_2^{\bullet} + CH_3(CH_2)_3SH \rightarrow PhCH_2{-}H + CH_3(CH_2)_3S^{\bullet} \quad (6)$$

(benzyloxy)methyl formate decrease from 16 ± 2 to 10 ± 1% (Table II); this result indicates that (benzyloxy)methyl formate is formed by at least two pathways, one involving cage recombination[24b] (shown by path c in Scheme I) and one involving free radical combinations in the bulk solution. Our product data imply that (benzyloxy)methyl formate is formed in 10 ± 1% yield by cage recombination; this ester therefore is formed in ca. 6% yield by pathways that involve noncaged radicals. A route to (benzyloxy)methyl formate formation from benzyl radical attack on ABO is shown by path h in Scheme I; a similar S_H2 chain process has been proposed as a step in the thermal decomposition of some alkyl peroxides.[28]

The decrease in yield of phenylacetaldehyde from 21 ± 2 to 11.0 ± 0.3% when ABO is decomposed in the presence of 1-butanethiol is consistent with either of two possibilities. Scheme I shows a pathway (path i) involving a chain process similar to path h, i.e., benzyl radical attack at the ozonide peroxide bond followed by single β-scission. In this case, however, β-scission occurs between the methine carbon and the ether oxygen of the ozonide ring, as shown in eq 7. The second explanation for the

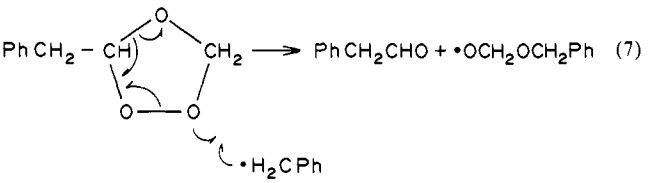

(7)

lower yield of phenylacetaldehyde postulates an acid-catalyzed thioacetalization to give **12** (eq 8).[29]

$$PhCH_2CHO + 2CH_3(CH_2)_3SH \overset{H^+}{\rightleftharpoons} \underset{\mathbf{12}}{PhCH_2CH(S(CH_2)_3CH_3)_2} + H_2O \quad (8)$$

Spin-Trapping Studies. Our results, the first data on the use of ESR spin trapping in the thermal decomposition of a Criegee ozonide, show that ABO decomposes at 37 °C to yield both oxygen- and carbon-centered radicals. Benzyl radicals are trapped by both DMPO and M_4PO; benzyl radical production is consistent with the mechanism presented in Scheme I. We have also shown that ABO decomposes to yield spin adducts with hfsc that are consistent with alkoxyl, acyl, and oxygen-centered radicals. The exact structure of all of these spin adducts cannot be assigned however.

Conclusion. Our results from product and ESR spin-trapping studies are consistent with the formation of benzyl and oxygen-centered radicals during the thermal decomposition of ABO. The mechanism shown in Scheme I involves the unimolecular homolysis of the ozonide peroxide bond followed by β-scission to yield, in part, benzyl radicals. That ABO peroxide bond homolysis and subsequent β-scission occur in a stepwise fashion is supported by the fact that the rates for thermal decomposition of OTO (E_a = 26.6 ± 0.5 kcal mol^{-1} and log A = 12.5 ± 0.3) are similar to rates obtained for the decomposition of ABO (E_a = 28.2 ± 0.3 kcal mol^{-1} and log A = 13.6).[5]

These findings agree with other work from our laboratory[5] that shows ABO, a model PUFA ozonide, initiates the autoxidation of 18:2ME. We suggest that radicals from the thermal decompositidon of Criegee ozonides may be a contributing pathway to the overall production of free radicals when PUFA are ozonized.

Acknowledgment. This work was supported in part by NIH Grant HL-16029 and by a contract with the National Foundation for Cancer Research. We also thank Dr. John P. Cosgrove and Dr. David H. Giamalva for helpful suggestions throughout this study and Brad Mayfield for technical assistance.

(23) Greiner, A.; Muller, U. *J. Prakt. Chem.* **1962**, *15*, 313–321.
(24) (a) Noyes, R. M. *J. Chem. Phys.* **1965**, *22*, 1349–1359, and references therein. (b) Koenig, T.; Fischer, H. In *Free Radicals*; Kochi, J., Ed.; Wiley: New York, 1973; Vol. I, pp 157–189.
(25) Nangia, P. S.; Benson, S. W. *Int. J. Chem. Kinet.* **1980**, *12*, 43–53.
(26) For instance, path j (Scheme I) shows radical attack on phenylacetaldehyde followed by rapid decarbonylation.
(27) Pryor, W. A. *Free Radicals*; McGraw-Hill: New York, 1966; p 133.
(28) (a) Drew, E. H.; Martin, J. C. *Chem. Ind.* **1959**, 925–926. (b) Doering, W. E.; Okamoto, K.; Krauch, H. *J. Am. Chem. Soc.* **1960**, *82*, 3579–3582. (c) Goh, S. H.; Huang, R. L.; Ong, S. H.; Sieh, I. *J. Chem. Soc. C* **1973**, 8205–8206. (d) Goh, S. H. *J. Org. Chem.* **1972**, *37*, 3098–3101. (e) Denney, D. B.; Feig, G. *J. Am. Chem. Soc.* **1959**, *81*, 5322–5324. (f) Pryor, W. A.; Pultinas, E. P. *J. Am. Chem. Soc.* **1963**, *85*, 133–136. (g) Pryor, W. A.; Pickering, T. L. *J. Am. Chem. Soc.* **1962**, *84*, 2705–2711.
(29) Although we did not analyze for **12**, we do observe the analogous product **13**

$$CH_3(CH_2)_5CHO + 2CH_3(CH_2)_3SH \overset{H^+}{\rightleftharpoons} \underset{\mathbf{13}}{CH_3(CH_2)_5CH(S(CH_2)_3CH_3)_2}$$

when OTO is decomposed in the presence of excess 1-butanethiol under similar conditions. Heptaldehyde is a major product from the thermal decomposition of OTO (ref 23 and unpublished data).